Interpretation of Single-Crystal Vibrational Spectra and Entropy of Pyrope and Almandine Using a Rigid-Ion Lattice-Dynamical Model

Carlo Maria Gramaccioli*,† and Tullio Pilati‡

Dipartimento di Scienze della Terra, Università, Via Botticelli 23, I-20133 Milan, Italy, and CNR, Istituto di Scienze e Tecnologie Molecolari, Via Golgi 19, I-20133 Milan, Italy

Received: October 23, 2002

For two silicates with the garnet structure, $Mg_3Al_2Si_3O_{12}$ (pyrope) and $Fe_3Al_2Si_3O_{12}$ (almandine), a rigid-ion lattice-dynamical model provides good agreement with the observed vibrational spectra. On examining the estimates of thermodynamic functions, as derived from the calculated phonon density of states, the agreement of entropy with the calorimetric data reported in the literature is not as satisfactory as that for other garnets. The situation can be notably improved at all temperatures in a most simple way if an order−disorder equilibrium concerning the distribution of the Mg or Fe atoms around their sites is assumed to take place; the variation of such equilibrium with temperature accounts for a sluggish "order−disorder" transition around 100 K.

1. Introduction

In recent years the study of the vibrational spectra of single crystals in comparison with lattice-dynamical estimates derived from atom−atom empirical potentials has led to a substantially improved interpretation of these spectra in solids; furthermore, the extent of application of such empirical potentials and their validity can be checked, also in view of better performances.

Following our interest in the field, which started from molecular crystals,[1−3] we tried to extend our Born−von Karman lattice-dynamical calculations to inorganic crystals of ionic character, many of which exist in nature as minerals. Here, we considered an extensive series of compounds, including oxides, silicates, and carbonates.[4−17] In all these cases, for the sake of relative simplicity, a rigid-ion model was used.

Our calculations involved the whole Brillouin zone, so that, in addition to Raman- and infrared-active vibrational frequencies, estimates of several physical properties depending on the phonon density of states could also be verified; among these properties, particularly important are thermodynamic functions such as entropy and the heat capacity in a wide range of temperature, as well as atomic displacement parameters (crystallographic "ADPs").

All these theoretical estimates were always shown to be in good to excellent agreement with the corresponding experimental data. Therefore, such a satisfactory behavior of atom−atom potentials has confirmed the practical possibility of using them to obtain reasonable estimates not only of "first-law" functions such as energy or enthalpy but also of "second-law" functions such as entropy and free energy. As a consequence, on improving such estimates, there is a reasonable prospect of their eventual application to interpreting chemical equilibria in solids at different temperatures or phase transitions.

On applying the same procedures to silicate garnets, satisfactory results in line with the others were obtained for Ca-rich terms, such as $Ca_3Al_2Si_3O_{12}$ (grossular) and $Ca_3Fe_2Si_3O_{12}$ (andradite). Instead, if Ca is replaced by Mg or Fe, as for $Mg_3Al_2Si_3O_{12}$ (pyrope) and $Fe_3Al_2Si_3O_{12}$ (almandine), the agreement with the experimental data (in particular, entropy) was notably inferior; here, the situation at and above room temperature could be notably improved in practice if the possibility of a low-temperature order−disorder transition concerning the Mg or Fe atoms was considered.[9]

The complexity of the problem suggested further investigation, on one hand, to improve the picture of the available experimental data or, on the other hand, in quest of a reasonable heuristic model affording a better agreement of thermodynamic estimates with their experimental counterparts, including the low-temperature region in proximity to the order−disorder transition. Furthermore, the performance of a model considering a *free-energy* minimum with respect to that of a model considering minimum energy has also been taken into account, at least as a potential future development in dealing with such complex cases.

2. Procedure of Calculation

Our calculations proceed according to the classic rigid-ion lattice-dynamical model and follow a well-established scheme.[2,4] Using a set of empirical atom−atom functions derived from the best fit to the vibrational frequencies of a group of oxides and silicates (see Table 1), the second derivatives of the potential energy with respect to the mass-weighted atomic shifts are evaluated; then, the so-called dynamical matrices are obtained by summing the corresponding derivatives multiplied by $\exp(-i\mathbf{q}\mathbf{r}_{p-p'})$, where $\mathbf{q}$ is the wave vector and $\mathbf{r}_{p-p'}$ is the distance vector between the atoms p and p' concerned; for the Coulombic contributions, a summation over the reciprocal lattice has been adopted.[18]

As a result of these calculations, besides the optically active vibrational frequencies and their interpretation, if the wave vector $\mathbf{q}$ is varied all over the Brillouin zone, the phonon density of states $g(\nu_i)$ can also be obtained: for this purpose, in our works a particular "uneven" sampling reduces the number of

* Corresponding author. E-mail: carlo.gramaccioli@unimi.it.
† Dipartimento di Scienze della Terra, Università.
‡ CNR, Istituto di Scienze e Tecnologie Molecolari.

10.1021/jp0222954 CCC: $25.00
Published on Web 05/13/2003

TABLE 1: Empirical Potentials Used Here

Atomic Charge (Electrons); O Calculated by Difference with Respect to the Charge Balance

Si	Mg	Fe	Al
−1.418	−1.482	−1.097	−1.286

Stretching Potentials: Energy (kJ/mol) = $A\{\exp[-2B(r-C)] - 2\exp[-B(r-C)]$

	A	*B*	*C*
Si−O	2798.03	0.756 24	1.641 73
Mg−O	58.0805	1.503 04	2.304 94
Fe−O	73.7643	1.489 95	2.208 57
Al−O	264.3066	1.374 06	1.909 97
O···O (<5.50)	5.97077	0.851 46	3.676 60

Bending Potentials for the Bond Angle β: K (mdyn/rad^2) = $A + B\cos\beta + C\cos^2\beta$

	A	*B*	*C*
O−Si−O	0.125 69	−0.625 73	1.117 16
O−Al−O	0.482 90	0.659 45	0.047 47
O−Mg−O	0.164 46	−0.090 38	−0.318 14
O−Fe−O	0.038 89		
Si−O−Si	0.138 83		
Al−O−Al	0.120 07		
Si−O−Al	0.181 20		

Bending−Stretching Potentials K (mdyn·rad) = $A + B(\beta - 109.47)$ (β in deg)

	A	B
O−Si−O/Si−O	0.100 91	−0.054 80
O−Al−O/Al−O	0.140 44	−0.001 49

Stretching−Stretching Potentials K (mdyn)

Si−O/Si−O	0.115 38
Al−O/Al−O	0.047 44

points in the Brillouin zone to be considered to about a hundred, thereby saving computing time very notably.[19,20]

From the density of states (with the normalizing condition: $\sum_i g(\nu_i)\Delta\nu_i = 1$), the estimates of thermodynamic functions can be derived, according to well-known expressions in statistical mechanics:

$$E = \sum_i g(\nu_i)\Delta\nu_i h\nu_i\{^1/_2 + [\exp(h\nu_i/kT) - 1]^{-1}\}$$

$$S = E/T - 3kN\sum_i g(\nu_i)\Delta\nu_i \ln[1 - \exp(h\nu_i/kT)]$$

$$C_v = 3R\sum_i g(\nu_i)\Delta\nu_i(-h\nu_i/kT)^2 \exp(h\nu_i/kT)/[\exp(h\nu_i/kT) - 1]^{-2}$$

where E, S, and C_v are the molar estimates of vibrational energy, entropy, and specific heat at constant volume, respectively, k and h are the Boltzmann and the Planck constants, N is Avogadro's number, and T is the absolute temperature.

A similar procedure holds for the theoretical evaluation of the crystallographic atomic displacement parameters or "ADPs" (as **U**'s); here, in view of the anisotropy, *also the eigenvectors* are important:

$$\mathbf{U}(p) = [Nm(p)]^{-1}\sum_i (2\pi\nu_i)^{-2} E_i \mathbf{e}_i(p)\, \mathbf{e}_i(p)^{*T}$$

where E_i is the mean energy of the vibrational mode, $\mathbf{e}_i(p)$ is the mass-adjusted polarization vector of the atom p, that is, the portion concerning this atom (three components) of the ith eigenvector ξ_i of the dynamical matrix corresponding to the mode, and $m(p)$ is the atomic mass; here, owing to vibrational anisotropy, rather than being over the density of states, the summation $\sum_i$ is extended to all the modes in the whole Brillouin zone.[21]

3. Vibrational Frequencies

Observed values for the Raman- and infrared-active fundamentals of pyrope and almandine are reported in Tables 2 and 3, respectively, together with the corresponding calculated values. Here, the experimental data reported in refs 22 and 23, which were the basis for reference in our former work,[9] have been implemented with new data obtained by Hofmeister et al. and with additional Raman measurements.[24] With respect to our previous results,[9] there are only a few variations: for instance, for pyrope the value of an E_g frequency now reported as 309 instead of 342 cm^{-1} is in much better agreement with our lattice-

TABLE 2: Frequencies (cm^{-1}) for Infrared- or Raman-Active Modes in Pyrope at Room Temperature

								T_{1u} (TO)									
obs[22]	140	200	238	260	279	339	365	385	423	458	478	536	583	664	878	906	976
obs[23]	134	195	221	259	336?	336	383	422	455	478		535	581	650	871	902	972
calc[9 a]	162	205	249	277	317	363	380	397	441	457	506	526	545	620	887	934	955
calc[25]	153	170	231	235	273	317	381	417	432	476	494	556	611	681	841	878	974
								T_{1u} (LO)									
obs[22]	152	218	240	263	280	353	370	400	422?	474?	528?	556	618	667	889?	940	1063
obs[23]	152	218	223	263	357	357	400	423		475	530	557	620	650	890	941	1060
calc[9 a]	164	209	257	300	319	370	400	404	453	497	557	526	610	642	898	957	1015
calc[25]	156	173	231	257	273	319	402	432	443	486	532	610	636	710	877	913	1068
								T_{2g}									
obs[23]	208	230	272	285	318		350	379	490	510	598	648	866	899	1062		
Chopelas[b]	208	?		300−310	318	342	347	380	490	510	598	647	866	899	1062		
obs[33 c]		222		322			353	383	492	512	598	650	871	902	1066		
calc[9 a]	166	185	259	318	334		368	403	475	546	638	671	891	937	1027		
calc[25]	193	227	247	297	323		353	367	473	515	607	644	844	876	1062		
					E_g								A_{1g}				
obs[23]	203	342	365	439	524	626	911	938				362	562	925			
Chopelas[a]	206	309	379	439?	523	627	867	938				362	561	925			
obs[33 c]	211	344	375		525			945				364	563	928			
calc[9 a]	207	313	369	408	553	571	868	880				351	574	935			
calc[25]	207	308	364	431	507	633	816	943				343	524	851			

[a] Our calculated values[9] using potential no. 4. There are slight differences with respect to our older values, due to the introduction of additional terms in the Coulombic lattice sums, to improve convergence. [b] New Raman data, from Chopelas (personal communication, 1999). [c] Observed values by Kolesov and Geiger;[33] these authors only have observed an additional T_{2g} line at 135 cm^{-1} and an E_g line at 284 cm^{-1}.

TABLE 3: Frequencies (cm^{-1}) for Infrared- or Raman-Active Modes in Almandine at Room Temperature

									T_{1u} (TO)										
obs[23]	112	138	158	196	236		318	345	376	412	448	468	525	561	635	865	889	952	
calc[9] [a]		142	166	179	220	272	291	362	396	432	458	501	533	557	604	899	944	962	
									T_{1u} (LO)										
obs[23]	115	147	160	205	246		322	347	396	422	518	461?	534	597	638	923	882?	1038	
calc[9] [a]		143	168	185	230	273	298	364	398	437	518	473	538	588	616	908	962	1004	
									T_{2g}										
obs[23]	166	198	212	239	293	312	355	474	498	576	628	862	892	1032					
calc[9] [a]	138	180	202	225	326	354	365	459	537	622	652	900	948	1020					
					E_g								A_{1g}						
obs[23]	163	326	368	421	521	593	910	920				347	553	910					
calc[9] [a]	170	275	346	396	529	554	858	891				343	563	920					

[a] Calculated values[9] using potential no. 4.

dynamical calculations. Conversely, in the new measurements a T_{2g} frequency around 342 cm^{-1} should not be a fundamental; for almandine, there are only a few changes in the attribution of the observed frequencies.

The possibility of using a different potential set independent of fit to these particular substances has also been considered; this set ("BEST") was derived by the best fit to a series of oxides and silicates not including these garnets.[12] However, the results of these calculations are markedly inferior to our older ones, to the point that some estimated values according to "BEST" are irreconcilable with the observations, and for this reason none of them are reported in Table 2. For instance, the intermediate A_{1g} frequency calculated in this way for pyrope is nearly 100 cm^{-1} higher than the corresponding observed value. It may be interesting to note that for reasons of symmetry in garnets all the A_{1g} frequencies involve motion of the oxygen atoms only; such observations indicate the possibility of attaining potentials of more general use by accounting for the polarizability of these atoms (see also below).

In conclusion, the data in Tables 2 and 3 clearly show a lattice-dynamical interpretation of the vibrational spectra of pyrope and almandine based on atom−atom potentials to be satisfactory; however, the interpretation of the vibrational spectra of garnets is not easy due to the notable number of atoms in the unit cell affording a thick distribution of vibrational frequencies, together with the possible presence of combinations, overtones, and also spurious peaks which are often encountered experimentally; for this reason, some details in the current interpretation of the spectra still need confirmation. Probably the most significant check of the validity of the model is provided by examining the A_{1g} modes, which are only three in number, and for this reason confusion is unlikely; here the agreement is indeed very good. Due to the particular symmetry of garnets, as we have seen, these vibrational modes imply oxygen atoms exclusively, but such atoms are linked to all the other atoms in the structure, thereby providing a test of more general value.

For pyrope, the most reliable agreement with the experimental data has obtained by Chaplin et al.[25] This work has been taken here as the best basis for interpreting the vibrational spectra; in any case, our own rigid-ion calculations provide comparable results, thereby justifying their extension to the whole Brillouin zone (see below). Since the potentials used by these authors were exclusively derived from the best fit to the spectra of other substances, their transferability has been confirmed. Here especially, rather than because of the slightly better agreement with the experimental data, the superior performance of Chaplin et al.'s results is evident; such a superiority is most probably due to having used a shell model to account at least partially for the polarizability of the oxygen atoms.

TABLE 4: Thermodynamic Functions for Pyrope (J/mol·K) at Different Temperatures[a]

T (K)	C_v(obs)	C_v(corr)[b]	C_v(vibr)	S(obs)	S(corr)[b]	S(vibr)
20	0.84	0.43	0.43	0.20	0.11	0.11
40	11.0	6.2	5.8	3.15	1.59	1.55
60	33.4	31.9	22.0	11.6	8.0	6.6
80	62.3	81.4	47.7	25.1	23.7	16.3
100	93.7	122.0	78.7	42.5	46.7	30.2
120	125.3	145.4	111.3	62.5	71.1	47.4
140	156.0	165.8	143.2	84.2	95.1	67.0
160	184.7	187.6	173.2	107.1	118.6	88.1
180	210.9	210.2	200.8	130.5	142.0	110.1
200	234.5	232.4	226.0	154.1	165.3	132.6
220	256.0	253.4	248.9	177.6	188.5	155.3
240	275.6	273.0	269.7	200.9	211.4	177.8
260	293.5	290.9	288.4	223.8	234.0	200.2
298	323.1	320.7	319.2	266.3	275.7	241.6
400	382.4	378.4	377.8	371.0	378.9	344.5
500	418.0	413.3	413.0	458.0	467.4	432.9
600	436.8	435.7	435.5	545.0	544.9	510.4
700	452.0	450.6	450.5	610.0	613.2	578.7

[a] Observed data from Haselton and Westrum,[28] and above 400 K from Tequi et al.[34] The C_v data have been obtained by subtracting $C_p - C_v = \alpha^2 TV\kappa$ from the observed values, using the physical constants reported by Hofmeister and Chopelas.[23] [b] The corrected values for the specific heat C_v and the entropy [C_v(corr) and S(corr), respectively] have been obtained by adding the equilibrium contribution due to disorder to the vibrational estimates [C_v(vibr) and S(vibr), respectively]. The corrected values are for $\Delta E = 4050$ J/mol.

Measurements of phonon dispersion curves for pyrope have been performed by Artioli et al.:[26] such results and the calculated values obtained by these authors are reported in Figure 1, together with our calculations; the agreement is quite good, thereby confirming the validity of our model.

4. Evaluation of Thermodynamic Functions at Low Temperature

Estimates of thermodynamic functions for pyrope and almandine are reported in Tables 4 and 5, respectively; in these tables, the purely vibrational contributions to the heat capacity and the entropy are reported in columns 4 and 7, respectively. Here, it is easy to notice that *at room temperature and higher temperatures* our purely vibrational estimates are *too low for entropy*, even if the contribution of magnetic spin disorder $\Delta S° = 3R \ln 5 = 40.14$ J/mol·K is added for almandine; instead, at these temperatures the calculated values of the *heat capacity (Figure 2) are always reasonable*, a point which provides additional evidence in favor of our vibrational model and potentials even in these cases, thereby excluding substantial influence of anharmonicity.

Because of the considerably smaller ionic radius of Fe^{2+} and Mg^{2+} with respect to that of Ca^{2+}, and since the "ideal" highly

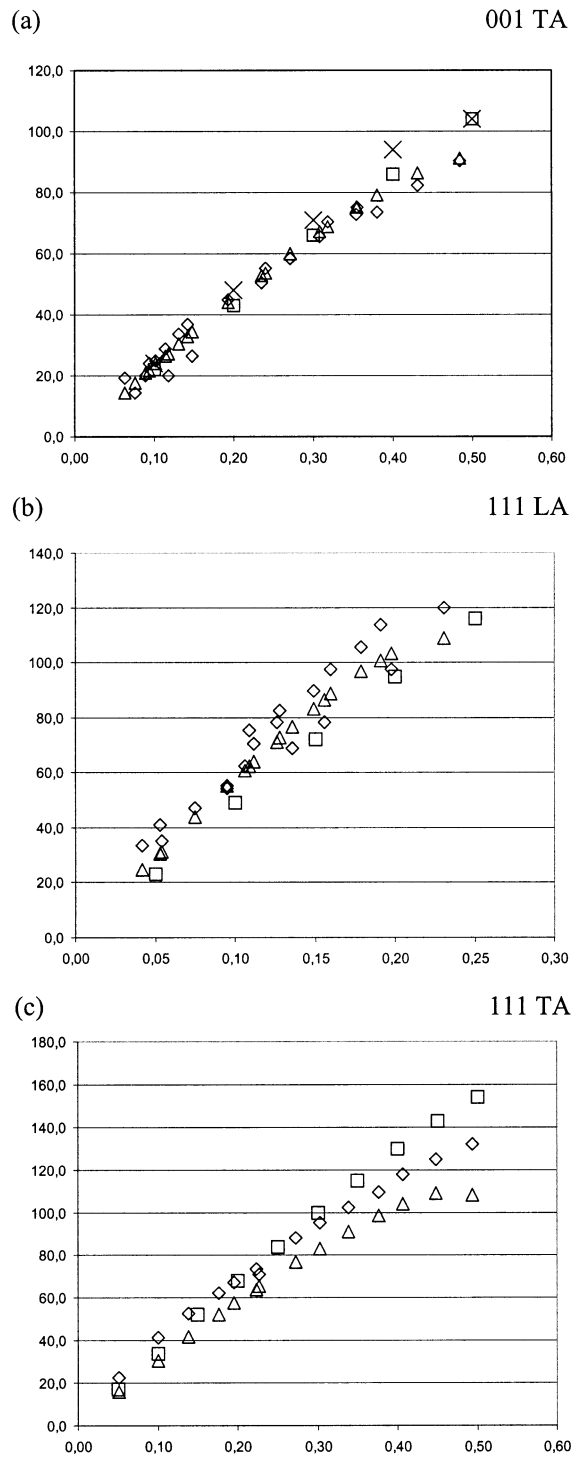

Figure 1. Acoustic phonon dispersion curves for pyrope: (a) transverse (TA) modes along [001]; (b) longitudinal (LA) modes along [111]; (c) transverse (TA) modes along [111]. The frequencies (vertical axis) are reported in cm^{-1}, whereas on the horizontal axes the fractions of the corresponding reciprocal *primitive* unit-cell distance are reported: triangles, calculated values by Artioli et al.;[26] diamonds, observed values by Artioli et al.;[26] squares and crosses, our calculations.

symmetric 24c site in the *Ia*3*d* group for all such atoms is more or less of the same size for all the garnet structures, for Ca-poor terms the possibility of configurational disorder becomes reasonable; such a possibility is connected with statistical displacement of the Mg or Fe atoms from their "ideal" position and might also explain the anomalous behavior of their ADPs as observed from crystallographic measurements.[9] On slightly

TABLE 5: Thermodynamic Functions for Almandine at Different Temperatures (J/mol·K)[a]

T (K)	C_v(obs)	C_v(corr)[b]	C_v(vibr)	S(obs)	S(corr)[b]	S(vibr)
10	16.2	56.0	0.1	23.8	19.8	0.0
15	15.0	19.3	0.2	30.1	35.5	0.1
20	14.3	6.6	0.8	34.3	38.9	0.2
30	16.6	5.2	4.0	40.4	40.9	1.0
40	24.7	12.1	11.5	46.2	43.1	3.1
50	36.3	23.5	22.1	52.9	47.0	6.8
60	50.0	41.9	36.7	60.7	52.9	12.1
70	64.7	65.2	52.1	69.5	61.2	19.1
80	80.2	92.5	68.4	79.2	71.6	27.0
100	111.8	143.6	101.9	100.5	97.8	45.7
120	143.3	175.2	134.3	123.8	127.1	67.2
140	173.4	195.4	164.9	148.2	155.8	90.3
160	201.5	213.9	193.2	173.3	183.1	114.2
180	227.4	233.0	219.2	198.6	209.4	138.5
200	250.9	252.3	242.9	223.8	232.1	160.0
220	272.6	271.2	264.5	248.8	256.8	183.9
240	292.8	288.8	284.0	273.5	281.3	207.9
260	311.6	306.0	302.4	297.7	306.1	232.4
280	328.4	321.1	318.3	321.5	329.4	255.5
298	341.9	333.6	331.4	342.6	349.9	275.8
325	360.6	350.9	349.2	373.0	379.8	305.5
350	373.7	364.9	363.6	400.4	406.3	331.9
400	396.5	397.3	396.5	451.8	454.9	380.4
420	403.7	396.6	395.9	471.0	474.8	400.3
500	429.5	423.0	422.6	544.3	546.1	471.5
600	453.0	445.4	445.1	625.1	625.7	551.0
700	470.6	460.7	460.5	696.5	695.7	621.0
800	483.7	470.8	470.7	760.6	758.5	683.8
1000	498.6	486.3	486.2	871.0	866.0	791.2

[a] Observed data from Anovitz et al.[31] The C_v data have been obtained by subtracting $C_p - C_v = \alpha^2 TV\kappa$ from the observed values, using the physical constants reported by these authors. [b] The corrected values for the specific heat and the entropy [C_v(corr) and S(corr), respectively] have been obtained by adding the equilibrium contribution due to disorder to the vibrational estimates [C_v(vibr) and S(vibr), respectively]. The corrected values are for $\Delta E = 4500$ J/mol and $\Delta E_{magn} = 450$ J/mol.

shifting the Mg or Fe atoms from the 24c site, four equivalent, symmetry-related sites would be involved, with consequent statistical occupation of $^1/_4$. Following such an assumption, complete configurational disorder would involve an entropy increase of $3R \ln 4 = 34.45$ J/mol·K; as a first approximation, by adding this contribution to our theoretical estimates, the corrected results became indeed in good agreement with the corresponding calorimetric data above 240 K.[9]

Without affirming that the "real" situation indeed corresponds to our inference, it might be interesting to extend such a heuristic procedure to low temperatures as well, for which disorder would not be complete. A very simple way of accounting for this situation could be the following:

Let us imagine there is equilibrium in the solid state between the disordered form and the ordered form. Accordingly, the partly disordered crystal can be considered to be a temperature-dependent equilibrium mixture of these two independent forms, as they were different substances; in view of their great chemical similarity, the vibrational spectrum can be considered to be practically identical for both of them, and the mixture to be an ideal solution. Therefore, the molar excess of entropy ΔS of the mixture with respect to that of the ordered form will be the following:

$$\Delta S = x\Delta S^\circ + \Delta S_{mix} = 3xR \ln 4 - R[x \ln x + (1 - x) \ln(1 - x)]$$

where $\Delta S^\circ = 3R \ln 4$ is the molar excess entropy of the pure disordered form with respect to the ordered counterpart, x is its molar fraction, and ΔS_{mix} is the entropy of mixing. At a given

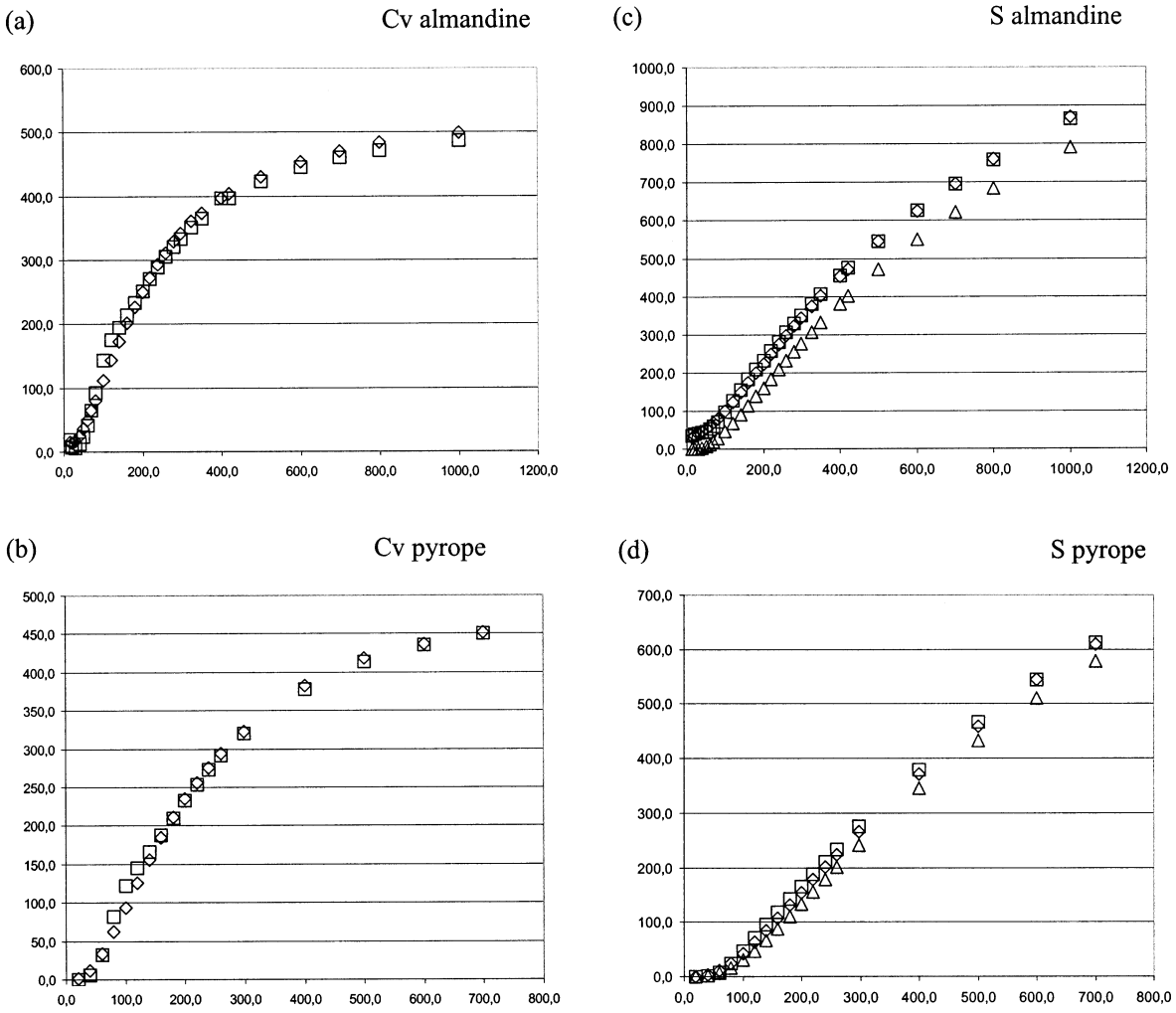

Figure 2. Heat capacities at constant volume (C_v) and values of entropy S (J/mol·K) for almandine and pyrope as a function of temperature (K): squares, calculated values; diamonds, observed values; triangles, purely vibrational contributions.

temperature, if both forms in the crystal are at equilibrium, it will be

$$[x]/[1-x] = K_{eq} = \exp(-\Delta F^{\circ}/RT) \approx \exp(-\Delta E/RT)\exp(\Delta S/R)$$

where ΔE is the excess energy of the "pure" disordered form with respect to that of the ordered form. Therefore, on assigning a certain value practically independent of temperature to ΔE, it is possible to deduce the molar fraction x and the correction ΔS to be added to the vibrational entropy at different temperatures; the results for pyrope are shown in column 5 of Table 4.

On comparing these results with the corresponding experimental data, the agreement becomes indeed reasonable, and at least in practice such a behavior approaches that of a sluggish "order−disorder transition" taking place at low temperature; a similar case can be observed in Table 5 for almandine (see below). Around the transition point, the process would actually involve anharmonic motion on its taking place, and for this reason our proposed model, although "harmonic", in some way accounts for anharmonicity, in a very simple way, at least in the transition region. It is interesting to remark that *such anharmonic behavior is important at low rather than at high temperatures*, in line with some crystallographic observations.[27]

A similar treatment can also be extended to dealing with magnetic disorder, although the approximation of having an ideal mixture might not be as satisfactory, in view of the different magnetic interactions between the ions; should such inconveniences occur in practice, in any case, they would be evident only for incomplete disorder of this kind, that is, at very low temperatures. Therefore, for almandine, according to our model, there should be *two* kinds of disorder, one magnetic and the other configurational, the latter deriving from partial occupation of sites around 24c.

Here, a rough assumption would be that the equilibrium constants K_{eq} between the "disordered" and the "ordered" magnetic form are the same for both the "site-ordered" and "site-disordered" form, and vice versa; therefore, the respective molar fractions x_0 and x_1 can be obtained independently, on applying the procedure shown above. Following the scheme for ideal solutions, the entropy of mixing should be the following:

$$\Delta S_{mix} = -R[y_1 \ln y_1 + y_2 \ln y_2 + y_3 \ln y_3 + y_4 \ln y_4]$$

where $y_1 = x_0x_1$, $y_2 = x_0(1 - x_1)$, $y_3 = x_1(1 - x_0)$, and $y_4 = (1 - x_0)(1 - x_1)$, since in this case there are four "substances", differing from each other on the grounds of order−disorder. Because the magnetic order−disorder transition occurs at much lower temperature than that concerning "static" disorder, the corresponding value of the excess energy (ΔE_{magn}) should be very low, and on the basis of the best fit of our model to almandine, it should be around 450 J/mol. In any case, since at temperatures around 30−40 K there is already almost complete

magnetic disorder, the inadequacies of such an approximation handling magnetic order−disorder transformations are not so important for most applications, and not at all for those at room and higher temperatures.

5. Discussion and Conclusions

This model implying the existence of temperature-dependent order−disorder equilibrium accounts for a *"nonvibrational" contribution to the specific heat*, so that especially in the proximity of the "transition points" the measured values are higher than those estimated by the harmonic model of lattice dynamics alone, in agreement with the character of a very sluggish higher-order phase transition. In this way, the observed "anomalously high heat capacity" observed for pyrope[22,28−29] might be explained; similar effects were also observed for almandine at low temperature.[31−32]

The reasonable behavior of our assumptions is shown in Tables 3 and 4 (see the third and sixth columns): here, the agreement with the observed data is satisfactory, especially at temperatures which are not too low.

The inferior performance of our model at very low temperatures is due to several factors. Apart from the approximations involved, the extrapolation of physical properties such as thermal expansion parameters or the bulk moduli may be critical, especially in proximity to transition points; such an inconvenience surely affects the experimental estimates of the specific heat at constant volume C_v, which are deduced from the corresponding values C_p actually measured at constant pressure. Moreover, our lattice-dynamical calculations have been performed using the crystal data at room temperature only.[10,12]

In some of our works[11] the possibility of using temperature-dependent crystal data has been considered in detail; a major difficulty arises because the values of bond lengths as they are obtained from crystallography should be corrected for thermal libration (a correction depending itself upon lattice dynamics) and the corresponding fit to spectroscopic data in deriving empirical potentials valid for all temperatures would become problematic. For this reason, we have adopted the present procedure, since all the other alternatives are far more complex and not completely convincing.

It is usually difficult to establish how much the use of room temperature data in the lattice-dynamical treatment could affect the derived estimates of thermodynamic quantities at low temperatures, since—apart from the theoretical difficulties outlined above which would render the results doubtful—for this purpose the calculations (which are already quite bulky) should be repeated, allowing variation of unit-cell parameters, as well as of the structural data. However, we do happen to have some information: for instance, at 100 K, for which structural data are available, using these data, the calculated value of vibrational entropy would be 27.7 instead of 30.2 cal/mol·K;[9] such a difference of 2.5 eu would result in a better agreement with the experimental estimate, although it is too small for believing that the observed disagreement in thermodynamic functions at low temperature can be fully explained in this way.

The disagreement between the observed and the calculated values of the heat capacity is often much higher than the corresponding $C_p - C_v$ difference; furthermore, considering that it occurs even for a non-antiferromagnetic substance such as pyrope, the reasons given above concerning thermal expansion parameters, the bulk moduli, or also the nonideality of the solid solution of different magnetic domains are not sufficient. On the other hand, it can be noticed that at these low temperatures *the agreement for entropy* (Tables 4 and 5) *is much better than that for the specific heat*; here, a plausible answer is that the experimental values of entropy actually result from an integration (in practice, a weighted average) of data at different temperatures. A definite possibility is that at very low temperatures equilibrium is very difficult to achieve in a "frozen" system, due to problems of activation energy; for this reason, the experimental data for the specific heat might not be entirely correct, and the errors are balancing each other when the experimental values for entropy are considered instead.

A further point should be considered: on shifting an atom from 24c to these "secondary" positions, *rather than energy, entropy may become instead the determining factor*. For instance, the probability density of some atomic positions corresponding to the *minimum free energy* conformation might show maxima *not necessarily* coinciding with positional energy minima; such a case is favored by the substantial increase in configurational entropy ($=3R \ln 4$) occurring when one atom is displaced from a high-symmetry position, so that the surrounding region is statistically occupied.

This might just be the case of pyrope and almandine, where the displacement of the atoms from the high-symmetrical 24c site implies a very low variation of packing energy, and especially so if the shift corresponds to a low-frequency normal mode: Here, despite the apparent "static disorder", the real situation might indeed correspond to a sophisticated case of anharmonic behavior, which is, however, far beyond the present status of the art to be exactly handled.

Therefore, although the "static disorder" invoked here might not necessarily correspond to "reality", it may become indeed a heuristic assumption, since a reasonable agreement with calorimetric data can be obtained. Such an assumption looks indeed reasonable, at least in view of the present difficulty in using more advanced theoretical ways to reproduce these experimental data.

Acknowledgment. The authors are grateful to Prof. Francesco Demartin and Alessandro Pavese and Mr. Luigi Saibene for useful suggestions and to Dr.Anastasia Chopelas for having provided us her latest set of Raman measurements on pyrope. The contribution of MURST ("40%": Project "Relazioni tra struttura e proprietà dei minerali: analisi ed applicazioni") is also gratefully acknowledged.

References and Notes

(1) Gramaccioli, C. M.; Filippini, G. *Chem. Phys. Lett.* **1984**, *108* (6), 585.
(2) Gramaccioli, C. M. *Int. Rev. Phys. Chem.* **1987**, *6* (4), 337.
(3) Filippini, G.; Gramaccioli, C. M. *Acta Crystallogr.* **1989**, *A45*, 261.
(4) Pilati, T.; Bianchi, R.; Gramaccioli, C. M. *Acta Crystallogr.* **1990**, *B46*, 301.
(5) Pilati, T.; Demartin, F.; Cariati, F.; Bruni, S.; Gramaccioli, C. M. *Acta Crystallogr.* **1993**, *B49*, 216.
(6) Pilati, T.; Demartin, F.; Gramaccioli, C. M. *Acta Crystallogr.* **1993**, *A49*, 473.
(7) Pilati, T.; Demartin, F.; Gramaccioli, C. M. *Acta Crystallogr.* **1994**, *B50*, 544.
(8) Pilati, T.; Demartin, F.; Gramaccioli, C. M. *Acta Crystallogr.* **1995**, *B51*, 721.
(9) Pilati, T.; Demartin, F.; Gramaccioli, C. M. *Acta Crystallogr.* **1996**, *B52*, 239.
(10) Pilati, T.; Demartin, F.; Gramaccioli, C. M. *Am. Mineral.* **1996**, *81*, 811.
(11) Pilati, T.; Demartin, F.; Gramaccioli, C. M. *Acta Crystallogr.* **1997**, *B53*, 82.
(12) Pilati, T.; Demartin, F.; Gramaccioli, C. M. *Am. Mineral.* **1997**, *82*, 1054.
(13) Pilati, T.; Demartin, F.; Gramaccioli, C. M. *Phys. Chem. Miner.* **1998**, *25*, 152.

(14) Pilati, T.; Demartin, F.; Gramaccioli, C. M. *Acta Crystallogr*. **1998**, *B54*, 515.
(15) Pilati, T.; Demartin, F.; Gramaccioli, C. M.; Pezzotta, F.; Fermo, P.; Bruni, S. *J. Phys. Chem.* **1998**, *102*, 4990.
(16) Pilati, T.; Demartin, F.; Gramaccioli, C. M. *Phys. Chem. Miner*. **1998**, *25*, 149.
(17) Gramaccioli, C. M.; Pilati, T. *Acta Crystallogr.* **2002**, *B58*, 965.
(18) Pilati, T.; Bianchi, R.; Gramaccioli, C. M. *Acta Crystallogr*. **1990**, *A46*, 309.
(19) Filippini, G.; Gramaccioli, C. M.; Simonetta, M. *Acta Crystallogr*. **1976**, *A32*, 259.
(20) Pilati, T.; Bianchi, R.; Gramaccioli, C. M. *Acta Crystallogr*. **1990**, *A46*, 485.
(21) Willis, B. T. M.; Pryor, A. W. *Thermal Motion in Crystallography*; Cambridge University Press: 1975; p 97.
(22) Hofmeister, A. M.; Chopelas, A. *Phys. Chem. Miner.* **1991**, *17*, 503.
(23) Hofmeister, A. M.; Chopelas, A. *Am. Mineral.* **1991**, *76*, 880.
(24) Hofmeister, A. M.; Fagan, T. J.; Campbell, K. M.; Schaal, R. B. *Am. Mineral.* **1996**, *81*, 418.
(25) Chaplin, T.; Price, G. D.; Ross, N. L. *Am. Mineral.* **1998**, *83*, 841.
(26) Artioli, G.; Pavese, A.; Moze, O. *Am. Mineral.* **1996**, *81*, 19.
(27) Artioli, G.; Pavese, A.; Ståhl, K.; McMullan, R. K. *Can. Mineral*. **1997**, *35*, 1009.
(28) Haselton, H. T.; Westrum, E. F. *Geochim. Cosmochim. Acta* **1980**, *44*, 701.
(29) Kieffer, S. W. *Rev. Geophys. Space Phys.* **1980**, *18*, 862.
(30) Geiger, C. A.; Armbruster, Th.; Lager, G. A.; Jiang, K.; Lottermoser, W.; Amthauer, G. *Phys. Chem. Miner*. **1992**, *19*, 121.
(31) Anovitz, L. M.; Essene, E. J.; Metz, G. W.; Bohlen, S. R.; Westrum, E. F., Jr.; Hemingway, B. S. *Geochim. Cosmochim. Acta* **1993**, *57*, 4191.
(32) Metz, G. W.; Anovitz, L. M.; Essene, E. J.; Bohlen, S. R.; Westrum, E. F., Jr.; Wall, V. J. *Trans., Am. Geophys. Union* **1983**, *64*, 346.
(33) Kolesov, B. A.; Geiger, C. A. *Phys. Chem. Miner*. **1998**, *25*, 142.
(34) Tequi, C.; Robie, R. A.; Hemingway, B. S.; Neuville, D.; Richet, P. *Geochim. Cosmochim. Acta* **1991**, quoted as "in press" by Hofmeister and Chopelas.[22]